7/16/96

Simultaneous observations of Polar Stratospheric clouds and HNO_3 over Scandinavia in January, 1992

S. T. Massie[1], M. L. Santee[2], W. G. Read[2], R. G. Grainger[3], A. Lambert[3], J. 1.. Mergenthaler[4], J. E. Dye[1], D. Baumgardner[1], W J. Randel[1], A. Tabazadeh[5], X. Tie[1], L. Pan[1], F. Figarol[1], F. Wu[1], and G. P. Brasseur[1]

Abstract. Simultaneous observations of Polar Stratospheric Cloud aerosol extinction and HNO_3 mixing ratios over Scandinavia arc examined for January 9-10, 1992. Data measured by the Microwave Limb Sounder (MLS), Cryogenic Limb Array EtaIon Spectrometer (CLAES), and improved Stratospheric and Mesospheric Sounder (ISAMS) experiments on the Upper Atmosphere Research Satellite (UARS) arc examined at locations adjacent to parcel trajectory positions. Regression coefficients, obtained from Mie calculations, arc used to transform aerosol extinctions into aerosol volume densities. Graphs of temperature versus volume density, and importantly, temperature versus HNO_3 mixing ratio, show volume increases and simultaneous loss of HNO_3 consistent with the presence of ternary solution droplets.

introduction

Polar Stratospheric Cloud (PSC) formation processes can be studied with data measured by the Upper Atmosphere, Research Satellite (lJARS), UARS instruments simultaneously observe both aerosol extinction and gas phase HNO_3, and thus it is possible to study the interconversion of gas phase HNO_3 into PSC particles. PSCs arc thought to be composed of either ice crystals (Type 11), nitric acid trihydrate (NAT) solid particles (Type la), or ternary

solution ($HNO_3/H_2SO_4/H_2O$) droplets (Type lb). Studies of forward scattering spectrometer probe (FSSP), balloonborne backscattersonde, and lidar data, have indicated the presence of ternary and NAT particles (*Tabazadeh et al., 1994a, Carslaw et al.*, 1994, *Drdla et Gil., 1994, Larsen et al.,* 1996).

Simultaneous UARS observations of aerosol extinction, measured by the Cryogenic Limb Array Spectrometer (CLAES) and Improved Stratospheric and Mesospheric Sounder (ISAMS) experiments, and gas phase HNO_3, measured by the CLAES and Microwave Limb Sounder (MLS) experiments, are used to study the formation of a PSC over Scandinavia during January 9-10, 1992. UARS observations on January 9 and 10 are used only if they are adjacent to specific parcel trajectories. The parcel positions originate over Greenland on January 9, and then proceed to a region of cold temperature, low HNO_3, and high aerosol extinction, located over Scandinavia on January 10.

Carslaw et al. (1994) used an equilibrium ternary model to show that the aerosol growth measured by the FSSP was consistent with HNO_3 uptake by ternary liquid droplets. The UARS extinction data are transformed into volume density values using regression coefficients, obtained from Mie calculations. Graphs of temperature versus volume density, and temperature versus gas phase HNO_3, reveal the interconversion between the gas and aerosol phase. The data are compared to equilibrium, and time dependent calculations, for PSCs of several compositions.

UARS Data

This study uses UARS observations at 46 and 68 hPa. CLAES and ISAMS aerosol extinction precision and accuracies for this range of pressure are on the order of 20 and 35% (*Massie et al.*,1996a, *Lambert et al.,1* 996). *Kumer et al.* (1 996) discuss the CLAES (version 7) data, and *Santee et al.* (1996) discuss the MLS (version 4) HNO_3 data, which are accurate

to 2 and 3 ppbv, respectively, at 46 hPa. MLS data at 68 hPa arc obtained by interpolation of 46 and 100 hPa retrieved measurements.

Since PSC microphysics is quite temperature dependent, it is important to assess the accuracy of the United Kingdom Mete.orological Office (UKMO) temperatures used in this study. Comparisons between the UKMO and radiosonde temperatures at pressures near 46 hPa for January 9-11, 1992 show that the UKMO temperatures arc 1 K warmer than the radiosonde temperatures for the 190 to 195 K temperature range, with an rms deviation of 2 K about the bias. UKMO temperatures were therefore decreased by 1 K.

'1'o transform the UARS extinction data into volume densities, Mie calculations are used to establish linear regression coefficients for each of the CLAES and ISAMS observational wavelengths. The Mie calculations use FSSP particle size distributions measured during the AASE II flights of the ER-2 (Dye *et al., 1992)* and sulfate aerosol size distributions measured over Laramie, Wyoming (*Deshler et al., 1993).* Regression coefficients were established for several sets of refractive indices (e.g, HNO_3/H_2O, H_2SO_4/H_2O and NAT) for various weight concentrations of HNO_3 and H_2SO_4. Binary HNO_3/H_2O indices approximate the $HNO_3/H_2O/H_2SO_4$ ternary indices, since the weight percent of H_2SO_4 is small in a ternary droplet for temperatures less than 195 K. For each extinction data point, the weight percent of H_2SO_4 and HNO_3 is calculated, the composition is specified to be either sulfate, ternary or NAT, and the appropriate set of regression coefficients arc then used to transform extinction to volume density. Details of the transformation calculations are discussed elsewhere (*Massie et al.,* 1996b).

UARS Data on January 9 - 10

Plate 1 displays mapped versions of UKMO temperatures (decreased by 1 K), CLAES HNO_3 mixing ratios, and ISAMS 12.1 μm extinction data, on the 460 K potential temperature surface for January 10, 1992. 1.OW mixing ratios and high extinction values arc

associated with a region of cold temperature over Scandinavia (see Figure 3 of *Taylor et al.*, 1994, for maps of temperature and aerosol extinction on adjacent days). Also displayed are specific parcel trajectories, calculated using UKMO wind field data. The parcels are located on the 460 K surface (corresponding to 19-20 km altitude over Scandinavia). Westernmost parcel positions, located over Greenland on January 9, have temperatures near 215 K, and easternmost positions over Norway on January 10 have temperatures near 190 K.

The volume densities presented in Figure 1 a arc an average of volume densities derived from ISAMS 12.1, ISAMS 6.23, CLAES 12.65, and CLAES 12.82 pm extinction data. UARS aerosol extinction and HNO_3 data at 46 and 68 hPa were linearly interpolated in pressure, to the pressure value of the nearest parcel trajectory point. 'l'he assigned temperature is that of the nearest trajectory point. Horizontal arrows indicate the ±2 K rms deviation between the UKMO temperatures and that of the radiosondes.

Time progresses from January 9 to January 10 from right to left for the observations displayed in Figure 1. An observation was used if the data point was within 400 km of a parcel trajectory position, on either the 9th or 10th. Figures 1a and 1 b display pairs of aerosol and HNO_3 data which were measured during the same 65 second UARS observation time period, i.e. the volume densities and HNO_3 mixing ratios arc simultaneous. Graphs (not shown) of only the data observed on the same clay as the trajectory points, show the same structure as in Figure 1, but contain fewer points.

In Figure 1 the aerosol is assumed to bc sulfate (H_2SO_4/H_2O droplets) for temperatures greater than 196 K, and assumed to be ternary droplets at temperatures less than 196 K. If the NAT composition is assumed at temperatures less than 196 K, then the volume densities are *20%* lower than in the ternary case. The temperature versus volume density graph (not shown), based upon the NAT indices, however, has a visual appearance similar to Figure 1a. The differences in refractive index do not alter the fact that the rise in volume density (with decreasing temperature) in Figure a occurs at a temperature less than that expected for a

NAT particle. The structure of Figure 1 a is controlled primarily by the relationship between temperature and aerosol extinction (e.g. see Figure 5 of *Taylor et al., 1994).*

Theoretical interpretation

Theoretical equilibrium curves, for NAT, nitric acid dihydrate (NAD) and ternary particles, are presented in Figures la-b, and are derived from the programs and data of *Tabazadeh et al* (1994b), *Carslaw et al.* (1995), and *Worsnop et al.* (1993). The four ternary theory curves were initialized with volume density values of 0.4 and 0.9 $\mu m^3 cm^{-3}$, and HNO_3 values of 9 and 13 ppbv The NAT and NAD curves were initialized with 0.9 μm^3 cm^{-3} and 13 ppbv. It is apparent that increases in volume density arc accompanied by decreases in gas phase HNO_3, that the four ternary curves for the HNO_3 gas phase overlap at colder temperatures, and that the theoretical curves for the NAT, NAD, and the ternary solutions have different temperature thresholds for uptake of HNO_3, and subsequent increases in the aerosol volume density.

Most of the data points in Figure 1 arc consistent with the existence of ternary solution droplets. The increase in volume density in Figure 1a, and the decrease in HNO_3 in Figure 1b, do not take place at the temperature threshold (i.e. 196 K) of the NAT equilibrium curve. These results arc in agreement with those of *Tabazadeh et al.* (1994a), *Carslaw et al. (1* 994) and *Drdla et al. (1994).*

A chemical box model is used to investigate the effects of heterogeneous reactions upon the gas phase HNO_3 mixing ratio. The box model uses the SMVGEAR solver (*Jacobson et* al., 1994), and contains 50 species, 150 reactions, and 16 heterogeneous reactions. The aerosol physical chemistry model (APCM) of *Tabazadeh et al.* (1994b) is used to calculate the equilibrium value of the volume density for the ternary solution droplets, which is used to estimate the area density (assuming a particle density of 2.5 particles/cm^3). For calculations

of the NAT particles, the mechanism of *Chipperfield et al. (1993)* is used. The volume and area densities are updated every 15 minutes.

Figure 1 c presents theoretical curves of HNO_3 versus temperature. Time is indicated at the top of the figure. The time dependent values in Figure 1 c were calculated using the temperatures and times from the parcel trajectory in Plate 1 which is closest to the equator, initial conditions for the calculations were derived from 2d model results, and the UARS observations. The calculations in Figure 1 c start with 5 ppmv H_2O, 7 ppmv HNO_3, 2,4 ppbv N_2O_5, 14 ppbv NOy, 1.7 ppbv C1ONO2, 1.7 ppbv HCl and 3.5 ppbv Cl_y.

The heterogeneous reactions

$$N_2O_5 + H_2O(\text{aerosol}) \rightarrow 2\ HNO_3 \quad (1)$$

$$ClONO_2 + H_2O(\text{aerosol}) \rightarrow HNO_3 + HOCl \quad (2)$$

$$ClONO_2 + HCl\ (\text{aerosol}) \rightarrow HNO_3 + Cl_2 \quad (3)$$

are influential in determining the gas phase HNO_3 mixing ratio. The "Ternary, all reactions" curve between O and 24 hours illustrates that reactions 1-3 enhance polar HNO_3 with a time scale of one day. The other theoretical curves show the results of the box model with and without heterogeneous reactions. Reaction (1) is the largest source term of gas phase HNO_3. Note that the equilibrium curves of Figure 1 b do not incorporate. chemical reactions, and are based upon thermodynamic (laboratory vapor pressure) data. The HNO_3 "Ternary, all reactions" solid curve values in Figure 1 c, at temperatures less than 195 K, are somewhat larger than the topmost ternary curve values in Figure 1 b. The "Ternary, all reactions" curve is supportive of the conclusion that the decrease of the observed HNO_3 is due to the uptake of gas phase HNO_3 into PSC droplets.

Comparison with other observations

The January period over Scandinavia has been studied by ground, aircraft, and satellite instrumentation. A comparison of UARS ClO, $ClONO_2$, HC1, and aerosol data on January

10, 1992 with a three dimensional model is discussed by *Geller et al. (1995). Geller et al. (1995)* demonstrate that heterogeneous processing transformed HCl and $ClONO_2$ into reactive chlorine (ClO).

Airborne FTIR observations, on January 9, of low HNO_3 column amounts west of Norway (67.6 "N, 9.5°E) by *Hopfner et al.* (1996) arc consistent with NAT particles, i.e. the observed HNO_3 column and the ECMWF temperature profile arc more consistent with the theoretical equilibrium HNO_3 column for NAT, than with that of the ternary solution. It is interesting to note that the lowest HNO_3 mixing ratios in Figure lb are within 600 km of the location of the Hopfner observations, and the data points arc closer to the NAT curves than to the ternary solution curves.

Schafer et al. (1994) report lidar observations at Andoya Island (69 "N, 16 °E), which is located along the coast of Norway, on January 5, 8, 9 and 19. The depolarization and perpendicular backscatter data on Janaury 9 support the presence of nonspherical PSC particles at altitudes above 20 km, and spherical particles below 20 km. Since the data presented in Figure 1b apply to the pressure range between 46 and 68 hPa, the data comes from the altitude range for which the lidar reports spherical particles. It is commonly held that nonspherical particles are solid "Type la NAT" particles, while spherical particles arc liquid "Type lb Ternary" droplets. The Schafer data at altitudes below 20 km, and the majority of the data points in Figures 1a and lb, arc consistent with the presence of ternary droplets.

Acknowledgements. This work was funded by the NASA UARS Guest Investigator Program by grant S-12899-F. The National Center for Atmospheric Research (NCAR) is sponsored by the National Science Foundation.

References.

Carslaw, K.S., *et al.*, Stratospheric aerosol growth and HNO_3 gas phase depletion from coupled HNO_3 and water uptake by liquid particles, *Geophys. Res. Lett.*, *21*, 2479-2482, 1994.

Carslaw, K. S., *et al.*, An analytic expression for the composition of aqueous HNO_3-H_2SO_4 stratospheric aerosols including gas phase removal of HNO_3, *Geophys. Res. Lett*, 22, 1877-18$0, 1995.

Chipperfield, M. P., D. Cariolle, P. Simon, R. Ramaroson, and D. J. Lary, A three-dimensional modeling study of trace species in the Arctic lower stratosphere during winter 1989-1990, *J. Geophys. Res.*, *98*, 7199-7218, 1993.

Deshler, T., *et al.*, Balloonborne measurements of Pinatubo aerosol during 1991 and 1992 at 41° N: Vertical profiles, size distribution, and volatility, *Geophys. Res. Lett.*, 20, 1435-1438, 1993.

Drdla, K., *et al.*, Analysis of the physical state of one Arctic polar stratospheric cloud based on observations, *Geophys. Res. Lett.*, 21, 2475-2478, 1994.

Dye, J. E., *et al.*, Particle Size Distributions in Arctic Polar Stratospheric Clouds, Growth and Freezing of Sulfuric Acid Droplets, and implications for Cloud Formation, *J. Geophys. Res.* ,97, 8015-8034, 1992.

Geller, M., *et al.*, UARS PSC, $ClONO_2$, HCl, and (10 measurements in early winter: Additional verification of the paradigm for chlorine activation, *Geophys. Res. Lett.*, 22, 2937-2940, 1995.

Hopfner, M., *et al.*, Evidence for the removal of gaseous HNO_3 inside the Arctic polar vortex in January 1992, *Geophys. Rcs. Left.*, 23, 149-152, 1996.

Jacobson, M. Z., and R. P. Turco, SMVGEAR: A sparse-matrix vectorized Gear code for atmospheric models, *Atmos. Environ.*, 28A, 273-284, 1994.

Kumer, J. B., *et al.*, Comparison of correlative data with nitric acid data version v7 from the Cryogenic Limb Array Etalon Spectrometer (CLAES) instrument deployed on the NASA

Upper Atmosphere Research Satellite (IJARS), *J. Geophys. Res.*, *101*, 9621-9656, 1996.

Lambert, A., *et* al., Validation of aerosol measurements by the Improved Stratospheric and Mesospheric Sounder, *J. Geophys. Res.*, 101, 9811-9830, 1996.

Larsen, N., *et* al., Balloonborne backscatter observations of type 1 PSC formation: Inference about physical state from trajectory analysis, *Geophys. Res. Lett.*, 23, 1091-1094, 1996.

Massie, S. T., et *al.*, Validation Studies Using Multi-wavelength CLAES Observations of Stratospheric Aerosol, *J. Geophys. Res.*, *101*, 9757-9733, 1996a.

Massie, S. T., *et al.*, Estimation of PSC volume and area densities from UARS extinction data, *J. Geophys.* Res. manuscript in preparation, 1996b.

Santee, M. J.., *et al.*, Polar vortex conditions during the 1995-96 Arctic winter: MLS C1O and HNO3, submitted to *Geophys. Res. Lett.*, 1996.

Schafer, et *al.*, Lidar observations of polar stratospheric clouds at Andoya, Norway, in January 1992, *Geophys. Res. Lett.*, *21*, 1307-1310, 1994,

Tabazadeh, A., *et* al., A study of Type 1 polar stratospheric cloud formation, *Geophys. Res. Lett.*, *21*, 1619-1622, 1994a.

Tabazadeh, A., *et al.*, A model for stydying the composition and chemical effects of stratospheric aerosols, *J. Geophys. Res.*, 99, 12897-12914, 1994b.

Taylor, F. W., et al., Properties of Northern Hemisphere Polar Stratospheric Clouds and Volcanic Aerosol in 1991/92 from UARS/SAMS Satellite Measurements, *J. Atm. Sci.*, 51, 3019-3026, 1994.

Worsnop, *et al.*, Vapor Pressures of Solid Hydrates of Nitric Acid: Implications for Polar Stratospheric Clouds, Science, 259, 71-74, 1993.

Figure and Plate captions.

Plate 1. Mapped fields on the 460 K potential temperature surface for January 10, 1992. a) UKMO temperature (decreased by 1 K). b) CLAES gas phase HNO_3 mixing ratios (ppbv). c) ISAMS 12.1 pm extinction (in units of 10-4 km^{-1}). d) Parcel trajectories on the 460 K surface. Parcel positions arc over Greenland on January 9, and over Scandinavia on January 10.

Figure 1. Profile data which arc adjacent to parcel trajectory positions on January 9 and January 10, 1992. a) Average values of ISAMS and CLAES volume densities. Equilibrium curves for ternary solution (solid lines), NAD and NAT solid particles (dashed lines) arc also presented. b) CLAES and MLS HNO_3 mixing ratios which correspond to the data points displayed in Figure 1a. The equilibrium curves for ternary solution (solid lines), NAD and NAT solid particles (dashed lines) are obtained from the same calculations which produced the theory curves in Figure 1a, c) Time dependent HNO_3 mixing ratios, calculated with and without heterogeneous reactions. Curve A incorporates all heterogeneous reactions, curve B only includes the $N_2O_5 + H_2O \rightarrow 2HNO_3$ reaction, curve C excludes all heterogeneous reactions, and curve D includes all heterogeneous reactions for the hTAT composition. Time values, indicated at the top of the graph, arc those of the parcels of the trajectory in Plate 1 which is closest to the equator.

---

1 NCAR, Boulder, Colorado

2 Jet Propulsion Laboratory, Pasadena, California

3 University of Oxford, Oxford, United Kingdom

4 Lockheed-Martin, Palo Alto, California

5 NASA-Ames, Moffitt Field, California

Corresponding author: S. T. Massic, NCAR, PO Box 3000, Boulder, CO, 80307.

(email: massie@ncar.ucar.edu)

January 10, 1992 460K

UKMET l(K) - 1K

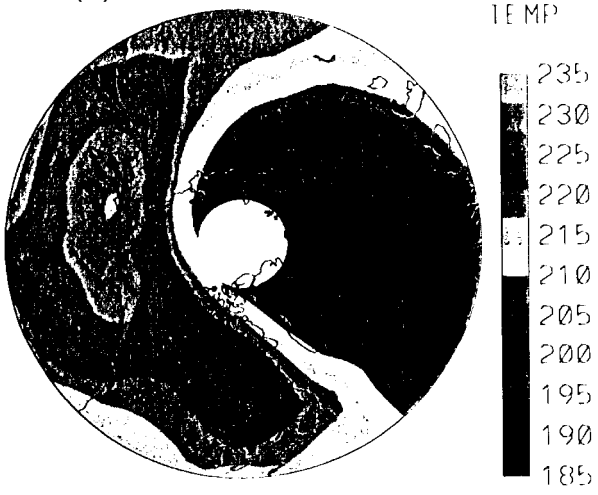

CLAES HN03 (PPBV)

ISAMS 12.1 micron extinction x 1E4

460K trajectories

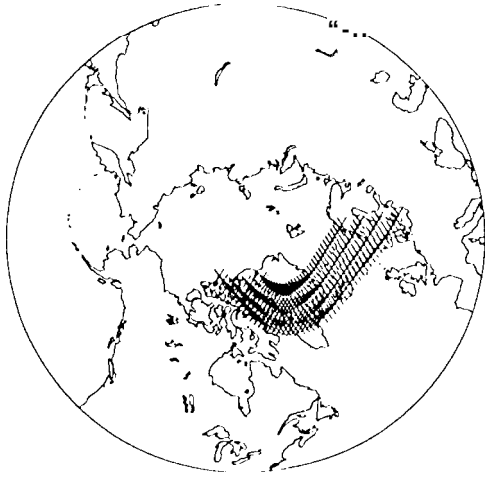

January 9-10, 1992
Theory (50 hPa, 9-13 ppbv HN03, 5 ppmv H20)

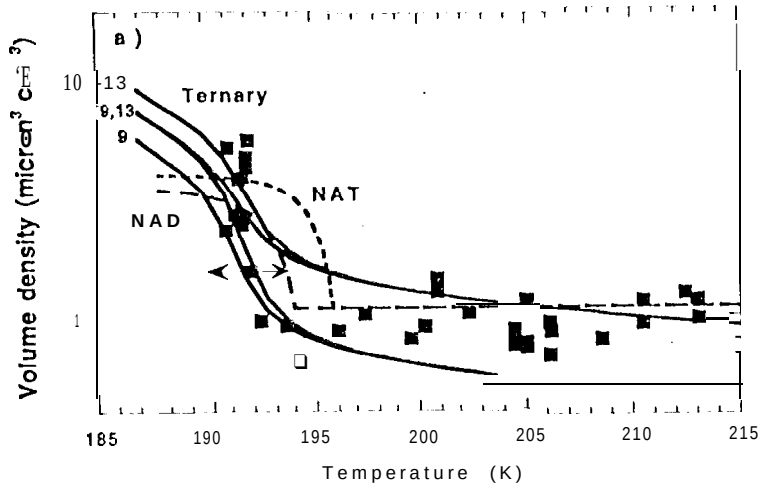

January 9-10, 1992
Theory (50 hPa, 9-13 ppbv HN03, 5 ppmv H20)

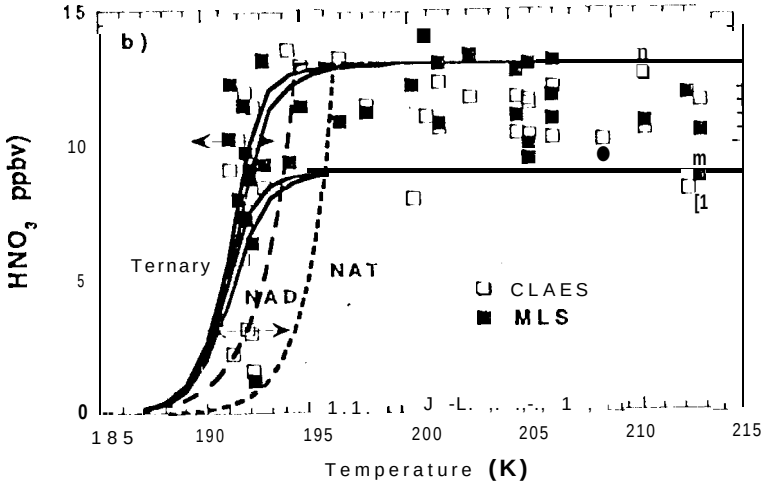

Time dependent calculations